Chapter 5
Theory of Three-Dimensional Dynamic Infinite Elements for Simulating Wave Propagation Problems in Infinite Media

Numerical simulation of infinite media is an important topic in dynamic soil–structure interaction problems. This topic arose from numerous practical problems, such as numerical simulation of building structural foundations, offshore structural foundations, dam foundations, nuclear power station foundations, just to name a few. The study of this topic becomes more important when the structure is large and the effects of earthquake waves are considered. Owing to the importance of dynamic soil–structure interaction effects, a large amount of research has been carried out in the past few decades (Elorduy et al. 1967; Lysmer and Kuhlemyer 1969; Kausel 1974; Zienkiewicz and Bettess 1975; Wong and Luco 1976; White et al. 1977; Cundall et al. 1978; Chow and Smith 1981; Hamidzadeh-Eraghi and Grootenhuis 1981; Medina and Taylor 1983; Liao et al. 1984; Wolf 1985, 1988; Zhao et al. 1987, 1989; Zhang and Zhao 1987; Zhao and Liu 2002, 2003). The general methodology of dealing with a dynamic soil–structure interaction problem is to divide the whole infinite foundation of the problem into a near field, which is comprised of a limited region of the infinite foundation, and a far field, which is comprised of the remaining part of the infinite foundation. As the near field is usually simulated by using the finite element method, both the geometrical irregularity and the non-homogeneity of an infinite foundation can be considered to determine the boundary of the near field. Since the far field is usually simplified as an isotropic, homogeneous, elastic medium, its effect on the near field can be represented either by some special artificial boundaries (Lysmer and Kuhlemyer 1969; Kausel 1974; White et al. 1977; Cundall et al. 1978; Liao et al. 1984; Zhao and Liu 2002, 2003) or by some special elements (Ungless 1973; Zienkiewicz and Bettess 1975; Bettess 1977, 1980; Chow and Smith 1981; Medina and Taylor 1983; Zhao et al. 1987, 1989). Through applying these special artificial boundaries or elements on the interface between the near field and the far field, the effect of the far field on the near field can be considered in the corresponding computational models.

From the wave-propagation point of view, there are two typical kinds of problems: a kind of wave radiation problem and a kind of wave scattering problem. For a wave radiation problem, the vibration source of the problem is located within the interior region of the near field, while for a wave scattering problem, the vibration source of the problem is located within the exterior region of the near field.

C. Zhao, *Dynamic and Transient Infinite Elements*, Advances in Geophysical and Environmental Mechanics and Mathematics, DOI 10.1007/978-3-642-00846-7_5,

The artificial boundary technique works well for dealing with wave radiation problems in infinite foundations, but it often fails in solving wave scattering problems in infinite foundations. Since the seismic analysis of a structure can be treated as a wave scattering problem, it is very difficult, if not impossible, to use the artificial boundary technique for solving dynamic soil–structure interaction problems, where earthquake waves are coming from the far fields of structural foundations. In such a case, the use of special elements such as dynamic infinite elements and boundary elements is a potential way for dealing with dynamic soil–structure interaction problems under earthquake loadings. Although the boundary element method is an efficient way to simulate wave scattering problems in a homogeneous medium due to a significant reduction in the total number of degrees-of-freedom of the system, the dynamic infinite element method is more suitable for simulating wave scattering problems in a non-homogeneous medium due to the banded and symmetrical nature of the resulting global mass and stiffness matrices of the system. On the other hand, for large structures such as arch dams, especially for double-curvature arch dams with smaller thicknesses and complicated configurations, a few finite elements are usually enough to simulate the thickness of a double-curvature arch dam so that the total number of degrees-of-freedom of the double-curvature arch dam cannot be greatly reduced when it is simulated using the boundary element method. In this case, the boundary element method loses its computational advantage in comparison to the finite element method, implying that for the seismic analysis of arch dams, the coupled computational method of finite elements and dynamic infinite elements (Zhao et al. 1989, 1992; Zhao and Valliappan 1991, 1993d, e) is more appropriate for simulating both an arch dam and the infinite foundation.

The concept of static infinite elements was initially presented in the seventies of the last century (Ungless 1973; Bettess 1977). Further work was carried out to apply the coupled computational model of finite elements and static infinite elements to the solution of static problems in engineering practice (Beer and Meek 1981; Zhao et al. 1986). The fundamental idea behind construction of a static infinite element is either to derive a special element displacement shape function, which is the production of a Lagrange interpolation function and a decay function, or to use special mapping techniques to map the infinite element into a finite one. The same idea has been used to develop two-dimensional dynamic infinite elements (Chow and Smith 1981; Medina and Taylor 1983; Zhao et al. 1987, 1992). Owing to the complicated mechanism of wave propagation in an infinite medium, the decay function for the static infinite element needs to be replaced by a wave propagation function for the dynamic infinite element. For simulating infinite solid media, several forms of two-dimensional dynamic infinite elements, which differ from the selection of the corresponding wave-propagation function of a dynamic infinite element, are presented by different authors (Chow and Smith 1981; Medina and Taylor 1983; Zhao et al. 1987, 1992). Nevertheless, early work on the development of dynamic infinite elements (Chow and Smith 1981; Medina and Taylor 1983) was mainly attributed to numerical simulation of two-dimensional and axisymmetrical wave radiation problems in infinite media. Although a previous three-dimensional dynamic infinite element (Zhao et al. 1989) was used to simulate a wavescattering problem for an arch dam–

foundation system, it has only one wavenumber so that it cannot be used to simulate efficiently and simultaneously wave-propagation problems of multiple wavenumbers (Zhao 1987). This means that for a given incident earthquake wave, one must first separate this wave into SH-wave, SV-wave and P-wave components and then use the wavenumber of each wave component to evaluate the stiffness and mass matrices of a dynamic infinite element. As a result, the stiffness and mass matrices of the previous three-dimensional dynamic infinite element need to be evaluated three times since only one wavenumber can be exactly represented each time by the previous three-dimensional dynamic infinite element.

Based on the above considerations, the theory of three-dimensional dynamic infinite elements is presented in this chapter. The wavenumbers of SH-waves, SV-waves and P-waves are used in the proposed three-dimensional dynamic infinite element. As a result, the coupled computational model of three-dimensional finite elements and three-dimensional dynamic infinite elements are better suited for simulating seismic wave propagation problems in the infinite foundations of arch dams. Owing to the use of a mapping technique in the process of developing the three-dimensional dynamic infinite element, it is feasible to use the coupled computational model of three-dimensional finite elements and three-dimensional dynamic infinite elements for dealing with dynamic arch dam–foundation interaction problems in a rectangular coordinate system. Two vibration problems, namely the vibration of a square rigid plate on a homogeneous elastic half-space and the vibration of a square rigid plate on a layered foundation, are considered as benchmark problems for the verification of the coupled computational model of three-dimensional finite elements and dynamic infinite elements.

5.1 Coupled Computational Model for Simulating Three-Dimensional Wave Propagation Problems in Infinite Foundations of Structures

For the numerical simulation of wave propagation problems in infinite foundations of structures, it is necessary to investigate the propagating mechanisms of harmonic waves in the infinite foundations of structures, because an arbitrary wave can be decomposed into the sum of several harmonic waves. The understanding of the detailed mechanisms of harmonic wave propagation in an infinite foundation can provide important insights into the fundamental behaviours and characteristics of a dynamic structure–foundation interaction system. After harmonic wave propagation problems in the infinite foundation are solved, the seismic analysis of a structure–foundation system can be straightforwardly carried out using the fast Fourier transform (FFT) and inverse Fourier transform (IFFT) techniques. Both the frequency domain method and the hybrid frequency-time domain method can be used for the linear and nonlinear dynamic analysis of a dynamic structure–foundation interaction system (Wolf 1985, 1988). Since an iteration technique is used for the hybrid frequency-time domain method, a nonlinear dynamic system, at each iteration, can

be approximately simulated as a linear one, so that the nonlinear effect of the dynamic system can be represented by pseudo-forces. These forces compensate for the difference between the internal forces obtained from the pseudo-linear system and those obtained from the original nonlinear system. The iteration can be continued until the convergence is achieved. For these reasons, harmonic waves are used to establish the theoretical basis of three-dimensional dynamic infinite elements in this section.

Assuming an infinite foundation is subjected to a harmonic loading and that the material of the infinite foundation exhibits hysteretic damping, the governing equations of wave motion of the system can be expressed as follows:

$$G^*\nabla^2 u + (\lambda^* + G^*)\left(\frac{\partial^2 u}{\partial x^2} + \frac{\partial^2 v}{\partial x \partial y} + \frac{\partial^2 w}{\partial x \partial z}\right) + f_x = \rho \frac{\partial^2 u}{\partial t^2}, \tag{5.1}$$

$$G^*\nabla^2 v + (\lambda^* + G^*)\left(\frac{\partial^2 u}{\partial x \partial y} + \frac{\partial^2 v}{\partial y^2} + \frac{\partial^2 w}{\partial y \partial z}\right) + f_y = \rho \frac{\partial^2 v}{\partial t^2}, \tag{5.2}$$

$$G^*\nabla^2 w + (\lambda^* + G^*)\left(\frac{\partial^2 u}{\partial x \partial z} + \frac{\partial^2 v}{\partial y \partial z} + \frac{\partial^2 w}{\partial z^2}\right) + f_z = \rho \frac{\partial^2 w}{\partial t^2}, \tag{5.3}$$

$$G^* = (1 + i\eta_d)G, \qquad \lambda^* = (1 + i\eta_d)\lambda, \tag{5.4}$$

where G is the shear modulus; λ is the Lamé constant; η_d is the hysteretic damping coefficient of the medium; u, v and w are the displacements in the x, y and z directions; f_x, f_y and f_z are the body force components in the x, y and z directions respectively; ρ is the density of the medium; ∇^2 is the second-order three-dimensional Laplace operator.

By making use of the Galerkin weighted residual method and neglecting the body forces in Eqs. (5.1), (5.2) and (5.3), the following discretized equations of wave motion of the system can be obtained:

$$-\omega^2[M]\{\Delta\} + (1 + i\eta_d)[K]\{\Delta\} = \{F_0\}, \tag{5.5}$$

where $\{\Delta\}$ is the unknown nodal displacement vector; ω is the circular frequency of a harmonic wave; $[M]$ and $[K]$ are the global mass and stiffness matrices of the system, respectively; and $\{F_0\}$ is the amplitude vector of the applied harmonic load. $[M]$, $[K]$ and $\{F_0\}$ can be assembled from the following element submatrices and subvectors:

$$[M]^e = \iiint_V [N]^T \rho [N] dV, \tag{5.6}$$

$$[K]^e = \iiint_V [B]^T [D^*][B] dV, \tag{5.7}$$

$$\{F_0\}^e = \iint_A [N]^T \{\overline{X}_0\} dA + [N]^T \{\overline{P}_0\}, \tag{5.8}$$

where V and A are the volume and surface area of the element; $\{\overline{X}_0\}$ is the amplitude vector of the element boundary traction; $\{\overline{P}_0\}$ is the amplitude vector of concentrated loads acting on the element; $[D^*]$ is the constitutive matrix of the element material; $[B]$ and $[N]$ are the strain matrix and shape function matrix of the element.

It needs to be pointed out that Eqs. (5.6), (5.7) and (5.8) are equally valid for both the finite and dynamic infinite elements. Although the volume of the dynamic infinite element can approach infinity, the mass and stiffness matrices of the element are still of finite values (Chow and Smith 1981; Medina and Taylor 1983; Zhao et al. 1987, 1989). This is because both the displacement shape function and strain matrices of the dynamic infinite element have a common term, known as the wave propagation function, whose value tends to zero as the volume of the dynamic infinite element approaches infinity. Since the derivation of three-dimensional finite element formulation is well known (Zienkiewicz 1977; Rao 1989), only the formulation of three-dimensional dynamic infinite elements is derived in the next section.

5.2 Formulation of Three-Dimensional Dynamic Infinite Elements

In terms of simulating a continuum system numerically, the continuous displacement field of the system is approximately represented by a discretized displacement field. The accuracy of the discretized model depends, to a large extent, on both the element size and the extent to which the displacement shape function of an element approaches the continuous displacement field of the original system. In the finite element analysis, the restriction of the construction of the displacement shape function for a finite element can be somewhat relaxed if a fine mesh of smaller elements is used to simulate the discretized system. However, the use of smaller elements can result in a significant increase in the total number of degrees-of-freedom of the discretized system so that both the computer CPU time and storage requirement for a given problem will increase remarkably. On the other hand, it is possible to construct an element using a more accurate displacement shape function to match the continuous displacement field of a real system so as to reduce significantly the total number of degrees-of-freedom of the discretized model of the system. This is the basic idea behind the construction of some special elements such as the finite strip element (Cheung 1976) and the boundary element (Brebbia 1978). When these special elements are used appropriately in the numerical simulation of a system, both computer CPU times and storage requirements are reduced significantly, compared with the finite element simulation of the same system. This basic idea is also applicable to the construction of a three-dimensional dynamic infinite element and, therefore, the key issue associated with the construction of a three-dimensional dynamic infinite element is how to choose an accurate displacement shape function for the element.

5.2.1 *Mapping Functions of Three-Dimensional Dynamic Infinite Elements*

To make the resulting three-dimensional dynamic infinite element more suitable for simulating both the geometrical irregularity and the material variety of a natural arch-dam foundation, a coordinate mapping technique is used to map a three-dimensional dynamic infinite element in the global coordinate system into a typical parent dynamic infinite element in the local coordinate system. Through the theoretical analysis of this typical parent dynamic infinite element, the mass and stiffness matrices of the three-dimensional dynamic infinite element can be derived.

For the three-dimensional dynamic infinite element shown in Fig. 5.1, the four sides of the infinite element in the direction of approaching infinity can be represented by straight lines, so that only eight nodes are sufficient to describe the geometry of the three-dimensional dynamic infinite element in the global coordinate system. However, to represent the wave propagation behaviour within the infinite element appropriately, 12 nodes are used to describe the displacement field of the three-dimensional dynamic infinite element. For this reason, the mapping relationship between the global coordinate system and the local coordinate system for the three-dimensional dynamic infinite element can be expressed as follows:

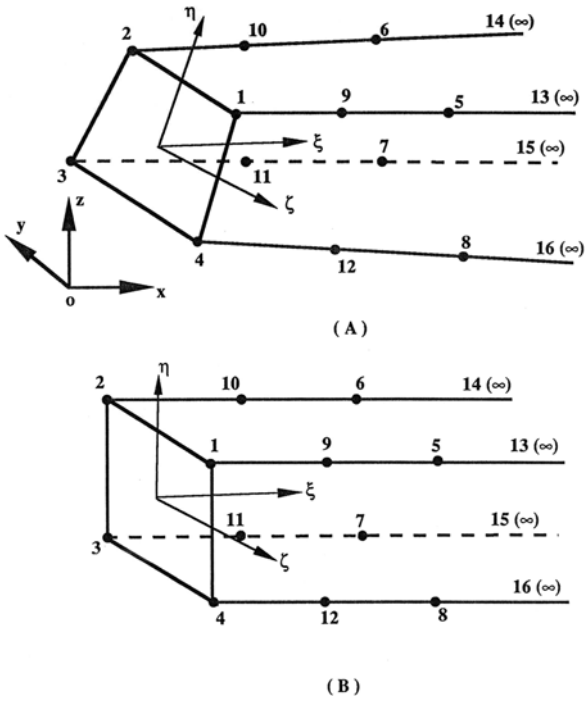

Fig. 5.1 Geometry of a three-dimensional 12-node dynamic infinite element: (**A**) the physical element; (**B**) the parent element

$$x = \sum_{q=1}^{8} M_q x_q, \tag{5.9}$$

$$y = \sum_{q=1}^{8} M_q y_q, \tag{5.10}$$

$$z = \sum_{q=1}^{8} M_q z_q, \tag{5.11}$$

where x_q, y_q and z_q are the nodal coordinates of the three-dimensional dynamic infinite element in the x, y and z directions, respectively; M_q ($q = 1,2, \ldots, 8$) is the mapping function of the three-dimensional dynamic infinite element.

$$M_1 = \frac{1}{4}(1-\xi)(1+\eta)(1+\zeta), \tag{5.12}$$

$$M_2 = \frac{1}{4}(1-\xi)(1+\eta)(1-\zeta), \tag{5.13}$$

$$M_3 = \frac{1}{4}(1-\xi)(1-\eta)(1-\zeta), \tag{5.14}$$

$$M_4 = \frac{1}{4}(1-\xi)(1-\eta)(1+\zeta), \tag{5.15}$$

$$M_5 = \frac{1}{4}\xi(1+\eta)(1+\zeta), \tag{5.16}$$

$$M_6 = \frac{1}{4}\xi(1+\eta)(1-\zeta), \tag{5.17}$$

$$M_7 = \frac{1}{4}\xi(1-\eta)(1-\zeta), \tag{5.18}$$

$$M_8 = \frac{1}{4}\xi(1-\eta)(1+\zeta). \tag{5.19}$$

Note that since the mapping functions of the three-dimensional dynamic infinite element are different from the displacement shape functions of the element, the three-dimensional dynamic infinite element is not an isoparametric element.

5.2.2 Displacement Shape Functions of Three-Dimensional Dynamic Infinite Elements

Consideration of the displacement compatibility condition on the connected interface between a three-dimensional eight-node isoparametric finite element (Zienkiewicz 1977) and a three-dimensional 12-node dynamic infinite element

(Zhao et al. 1993d) yields the following displacement field for the three-dimensional 12-node dynamic infinite element:

$$u = \sum_{q=1}^{12} N_q u_q, \tag{5.20}$$

$$v = \sum_{q=1}^{12} N_q v_q, \tag{5.21}$$

$$w = \sum_{q=1}^{12} N_q w_q, \tag{5.22}$$

where N_q (q = 1, 2, ..., 12) is the displacement shape function of the three-dimensional 12-node dynamic infinite element as follows:

$$N_q = P_q(\xi)\left[\frac{1}{4}(1+\eta)(1+\zeta)\right] \qquad (q = 1, 5, 9), \tag{5.23}$$

$$N_q = P_q(\xi)\left[\frac{1}{4}(1+\eta)(1-\zeta)\right] \qquad (q = 2, 6, 10), \tag{5.24}$$

$$N_q = P_q(\xi)\left[\frac{1}{4}(1-\eta)(1-\zeta)\right] \qquad (q = 3, 7, 11), \tag{5.25}$$

$$N_q = P_q(\xi)\left[\frac{1}{4}(1-\eta)(1+\zeta)\right] \qquad (q = 4, 8, 12), \tag{5.26}$$

where $P_q(\xi)$ (q = 1, 2, ..., 12) is the wave propagation function of the three-dimensional 12-node dynamic infinite element; N_q ($q = 1, 2, \ldots, 12$) is the displacement shape function of the three-dimensional 12-node dynamic infinite element. The wave propagation function of the three-dimensional 12-node dynamic infinite element can be determined by investigating the harmonic wave propagation behaviour in an infinite medium (Zhao and Valliappan 1993d). When an isotropic, homogeneous and elastic half-space is subjected to a harmonic loading, the induced harmonic waves propagate from the vibration source into the far field of the half-space. The analytical solution for this problem can be expressed using the special functions, known as Bessel functions and Hankel functions (Graff 1975; Medina and Taylor 1983). For example, for P-waves and S-waves propagating with spherical symmetry, the harmonic free-vibration solution for spherically symmetrical waves traveling in a homogeneous, isotropic and elastic medium, away from the origin of a vibration source, is expressed as follows (Medina and Taylor 1983):

$$u = B_1 h_1^{(2)}(k_p R), \tag{5.27}$$

$$v = B_2 h_0^{(2)}(k_s R), \tag{5.28}$$

$$w = B_3 h_0^{(2)}(k_s R), \tag{5.29}$$

$$R = \sqrt{x^2 + y^2 + z^2}, \tag{5.30}$$

where $h_0^{(2)}$ and $h_1^{(2)}$ are the zeroth order and first-order spherical Hankel functions of the second kind; B_1, B_2 and B_3 are three constants; k_p and k_s are the wavenumbers of a P-wave and an S-wave, respectively.

Note that the asymptotic behaviour of $h_0^{(2)}$ and $h_1^{(2)}$ can be expressed using the following equations (Graff 1975; Medina and Taylor 1983):

$$h_0^{(2)}(x) = \frac{1}{x} \exp\left[i\left(x - \frac{\pi}{4}\right)\right] + O\left(|x|^{-2}\right), \tag{5.31}$$

$$h_1^{(2)}(x) = \frac{1}{x} \exp\left[i\left(x - \frac{3\pi}{4}\right)\right] + O\left(|x|^{-2}\right). \tag{5.32}$$

Equations (5.27), (5.28), (5.29), (5.31) and (5.32) clearly indicate that the wave propagation behaviour in the far field of a half-space can be approximately represented by exponential functions. A similar conclusion can be obtained when a cylindrical Rayleigh wave (i.e. R-wave) propagating in a homogeneous, isotropic and elastic half-space is considered. Therefore, in the far field of a half-space, the asymptotic behaviour of these special functions can be approximately expressed as a combination of several exponential functions. The physical explanation for this is that the induced waves in the far field of the half-space can be approximately represented using the superposition of plane harmonic waves. Based on this recognition and consideration of induced waves with multiple wavenumbers, the general form of the wave propagation function for the three-dimensional 12-node dynamic infinite element can be expressed as

$$\begin{aligned} P_q(\xi) = \exp(-\alpha\xi) \left[c_1 \exp(-i\beta_1\xi) + c_2 \exp(-i\beta_2\xi)\right. \\ \left. + c_3 \exp(-i\beta_3\xi)\right] \quad (q = 1, 2, \ldots, 12), \end{aligned} \tag{5.33}$$

where α is the nominal decay coefficient that is used to express the wave amplitude attenuation due to both the wave energy dissipation in the three-dimensional 12-node dynamic infinite element and the geometrical divergence of the three-dimensional 12-node dynamic infinite element. Note that the determination of the value of α was addressed in Chap. 2. β_1, β_2 and β_3 are three nominal wavenumbers corresponding to R-, S- and P-waves in the three-dimensional 12-node dynamic infinite element. These nominal wavenumbers are used to express the phase characteristics of wave propagation in the three-dimensional 12-node dynamic infinite element. c_1, c_2 and c_3 are three constants to be determined by matching the displacement field of the three-dimensional 12-node dynamic infinite element with that of the infinite medium.

Although R-waves, S-waves and P-waves decay with distance from the point of excitation at different rates, previous studies (Zhang and Zhao 1987; Zhao et al. 1989) have demonstrated that the decay rates of different waves in a dynamic infinite

element are not sensitive to the numerical results. Thus, the same decay rate is used for all three waves involved in the construction of the wave propagation function of the three-dimensional 12-node dynamic infinite element. Regarding the exponential decay of the Rayleigh wave with the depth from ground surface, it is reasonable to represent this phenomenon approximately by using piecewise interpolation in the η and ζ directions for the three-dimensional 12-node dynamic infinite element.

To determine the constants c_1, c_2 and c_3, the displacement field of the three-dimensional 12-node dynamic infinite element needs to be considered. Letting nodal displacements for the nodes located at an infinite side in the ξ direction of the element be equal to the element displacement field expressed in Eqs. (5.20), (5.21) and (5.22), these three constants can be determined. For instance, if the side of the three-dimensional 12-node dynamic infinite element with nodes 1 ($\xi = 0$), 5 ($\xi = 1/2$) and 9 ($\xi = 1$) is considered, the following relationships emerge:

$$\begin{Bmatrix} u_1 \\ u_5 \\ u_9 \end{Bmatrix} = \begin{bmatrix} 1 & 1 & 1 \\ -\exp\left[-\frac{1}{2}(\alpha + i\beta_1)\right] & -\exp\left[-\frac{1}{2}(\alpha + i\beta_2)\right] & -\exp\left[-\frac{1}{2}(\alpha + i\beta_3)\right] \\ \exp\left[-(\alpha + i\beta_1)\right] & \exp\left[-(\alpha + i\beta_2)\right] & \exp\left[-(\alpha + i\beta_3)\right] \end{bmatrix} \begin{Bmatrix} c_1 \\ c_2 \\ c_3 \end{Bmatrix} = [C] \begin{Bmatrix} c_1 \\ c_2 \\ c_3 \end{Bmatrix}. \tag{5.34}$$

Solving Eq. (5.34) yields the following matrix equation:

$$\begin{Bmatrix} c_1 \\ c_2 \\ c_3 \end{Bmatrix} = [C]^{-1} \begin{Bmatrix} u_1 \\ u_5 \\ u_9 \end{Bmatrix} = [E] \begin{Bmatrix} u_1 \\ u_5 \\ u_9 \end{Bmatrix}. \tag{5.35}$$

After these three constants are determined, the wave-propagation function for the three-dimensional 12-node dynamic infinite element can be further expressed as follows:

$$P_q(\xi) = E_{11}\exp\left[-(\alpha + i\beta_1)\xi\right] + E_{21}\exp\left[-(\alpha + i\beta_2)\xi\right] + E_{31}\exp\left[-(\alpha + i\beta_3)\xi\right] \qquad (q = 1, 2, 3, 4), \tag{5.36}$$

$$P_q(\xi) = E_{12}\exp\left[-(\alpha + i\beta_1)\xi\right] + E_{22}\exp\left[-(\alpha + i\beta_2)\xi\right] + E_{32}\exp\left[-(\alpha + i\beta_3)\xi\right] \qquad (q = 5,6,7,8), \tag{5.37}$$

$$P_q(\xi) = E_{13}\exp\left[-(\alpha + i\beta_1)\xi\right] + E_{23}\exp\left[-(\alpha + i\beta_2)\xi\right] + E_{33}\exp\left[-(\alpha + i\beta_3)\xi\right] \qquad (q = 9, 10, 11, 12), \tag{5.38}$$

where

$$E_{11} = \frac{1}{\Delta}\exp\left[-\frac{1}{2}(3\alpha + i\beta_2 + i\beta_3)\right]\left[\exp\left(-\frac{i}{2}\beta_3\right) - \exp\left(-\frac{i}{2}\beta_2\right)\right], \tag{5.39}$$

$$E_{21} = \frac{1}{\Delta}\exp\left[-\frac{1}{2}(3\alpha + i\beta_1 + i\beta_3)\right]\left[\exp\left(-\frac{i}{2}\beta_1\right) - \exp\left(-\frac{i}{2}\beta_3\right)\right], \quad (5.40)$$

$$E_{31} = \frac{1}{\Delta}\exp\left[-\frac{1}{2}(3\alpha + i\beta_1 + i\beta_2)\right]\left[\exp\left(-\frac{i}{2}\beta_2\right) - \exp\left(-\frac{i}{2}\beta_1\right)\right], \quad (5.41)$$

$$E_{12} = \frac{1}{\Delta}\exp(-\alpha)\left[\exp(-i\beta_2) - \exp(-i\beta_3)\right], \quad (5.42)$$

$$E_{22} = \frac{1}{\Delta}\exp(-\alpha)\left[\exp(-i\beta_3) - \exp(-i\beta_1)\right], \quad (5.43)$$

$$E_{32} = \frac{1}{\Delta}\exp(-\alpha)\left[\exp(-i\beta_1) - \exp(-i\beta_2)\right], \quad (5.44)$$

$$E_{13} = \frac{1}{\Delta}\exp\left(-\frac{1}{2}\alpha\right)\left[\exp\left(-\frac{i}{2}\beta_3\right) - \exp\left(-\frac{i}{2}\beta_2\right)\right], \quad (5.45)$$

$$E_{23} = \frac{1}{\Delta}\exp\left(-\frac{1}{2}\alpha\right)\left[\exp\left(-\frac{i}{2}\beta_1\right) - \exp\left(-\frac{i}{2}\beta_3\right)\right], \quad (5.46)$$

$$E_{33} = \frac{1}{\Delta}\exp\left(-\frac{1}{2}\alpha\right)\left[\exp\left(-\frac{i}{2}\beta_2\right) - \exp\left(-\frac{i}{2}\beta_1\right)\right], \quad (5.47)$$

$$\begin{aligned}\Delta = {} & \exp\left(-\frac{3}{2}\alpha\right)\left\{\exp\left[-\frac{i}{2}(\beta_2 + \beta_3)\right]\left[\exp\left(-\frac{i}{2}\beta_3\right) - \exp\left(-\frac{i}{2}\beta_2\right)\right]\right\} \\ & + \exp\left(-\frac{3}{2}\alpha\right)\left\{\exp\left[-\frac{i}{2}(\beta_1 + \beta_2)\right]\left[\exp\left(-\frac{i}{2}\beta_2\right) - \exp\left(-\frac{i}{2}\beta_1\right)\right]\right\} . \\ & + \exp\left(-\frac{3}{2}\alpha\right)\left\{\exp\left(-\frac{i}{2}(\beta_1 + \beta_3)\right)\left[\exp\left(-\frac{i}{2}\beta_1\right) - \exp\left(-\frac{i}{2}\beta_3\right)\right]\right\}\end{aligned} \quad (5.48)$$

Note that a sufficient condition for the existence of $P_q(\xi)$ (q= 1, 2, . . ., 12) in the three-dimensional 12-node dynamic infinite element is that β_1, β_2 and β_3 are three different constants. This condition can be satisfied for simulating wave-propagation problems in an infinite medium, because, from the physical point of view, R-, S- and P-waves have three different wavenumbers in the infinite medium.

In addition, the following expression for the wave propagation function of the three-dimensional 12-node dynamic infinite element exists:

$$P_q(\xi_r) = \delta_{qr} \qquad (q = 1, 2, \ldots, 12;\ r = 1, 2, \ldots, 12), \quad (5.49)$$

where δ_{qr} is the Kronecker delta. This implies that for any displacement shape function, N_q (q = 1, 2, . . ., 12), $N_q = 1$ when $\xi = \xi_q$, $\eta = \eta_q$ and $\zeta = \zeta_q$, while $N_q = 0$ when $\xi = \xi_r$, $\eta = \eta_r$ and $\zeta = \zeta_r$, where $r \neq q$.

Supposing the velocities of the P-wave, S-wave and R-wave in an elastic infinite medium are 3000, 1500 and 1398 m s^{-1}, respectively, and that the excitation circular

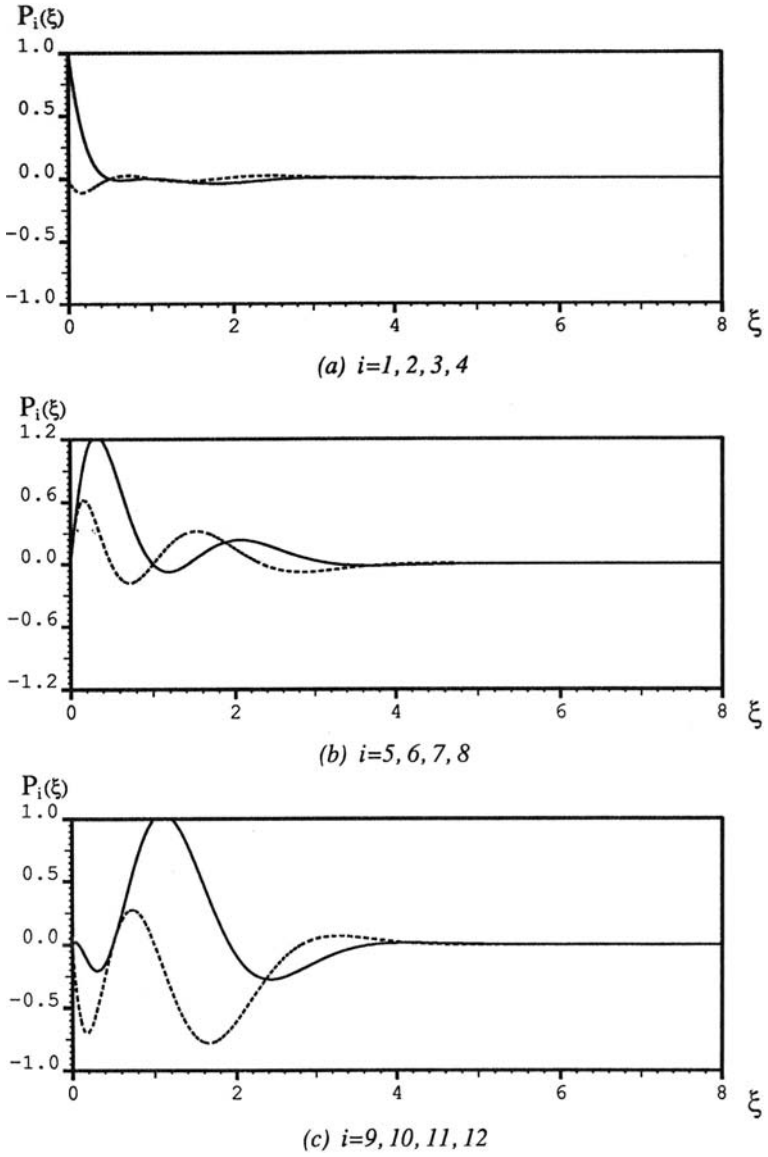

Fig. 5.2 Distributions of wave-propagation functions in a three-dimensional 12-node dynamic infinite element: the *solid lines* represent the real parts of the wave-propagation function, while the *dashed lines* represent the imaginary parts of the wave-propagation function

frequency is 30 rad s^{-1}, the corresponding wavenumbers for the P-wave, S-wave and R-wave are 0.01, 0.02 and 0.0215, respectively. If these wavenumbers are multiplied by 100, which means that the global coordinates of the three-dimensional 12-node dynamic infinite element is divided by 100 in the ξ direction, the distributions of the wave propagation functions (i.e. $P_q(\xi)$ $(q = 1, 2, \ldots, 12)$), which are used in the three-dimensional 12-node dynamic infinite element, are shown in Fig. 5.2, where $\alpha = 2.2$, $\beta_1 = 1$, $\beta_2 = 2$ and $\beta_3 = 2.25$. In this figure, the solid and dashed lines are the real and imaginary parts of the wave-propagation functions, which are used to express the element-displacement pattern for the three-dimensional 12-node dynamic infinite element. From the wave-propagation point of view, it is the wave-propagation function that describes how waves in the three-dimensional 12-node dynamic infinite element propagate from the element nodes to the far field of the infinite medium.

Another characteristic of the three-dimensional 12-node dynamic infinite element is that real (physical) wavenumbers in a global coordinate system can be adjusted by changing the locations of element side nodes 5, 6, 7 and 8 in the global coordinate system. This technique is helpful when the three-dimensional 12-node dynamic infinite element is used to simulate wave-propagation problems in non-homogeneous infinite foundations (Zhao et al. 1987, 1989).

5.2.3 *Mass and Stiffness Matrices of Three-Dimensional Dynamic Infinite Elements*

If the same procedures as those used in the finite element method (Zienkiewicz 1977; Zhao et al. 1992) are used, both the mass matrix and the stiffness matrix of the three-dimensional 12-node dynamic infinite element can be expressed as follows:

$$[M]^e = \int_{-1}^{1}\int_{-1}^{1}\int_{0}^{\infty} [N]^T \rho [N] \, |J| \, d\xi d\eta d\zeta , \tag{5.50}$$

$$[K]^e = \int_{-1}^{1}\int_{-1}^{1}\int_{0}^{\infty} [B]^T [D^*][B] \, |J| \, d\xi d\eta d\zeta , \tag{5.51}$$

where $[B]$ and $[N]$ are the strain matrix and shape function matrix of the three-dimensional 12-node dynamic infinite element; $[D^*]$ is the constitutive matrix of the element material; $|J|$ is the Jacobian determinant which can be determined using the mapping relationship of the element (in Eqs. (5.9), (5.10) and (5.11)); and ρ is the density of the element material.

To determine the shape function matrix, Eqs. (5.20), (5.21) and (5.22) can be written in the matrix form:

$$\begin{Bmatrix} u \\ v \\ w \end{Bmatrix}^e = [N] \{\Delta\}^e , \tag{5.52}$$

where $[N]$ is the shape function matrix of the three-dimensional 12-node dynamic infinite element; $\{\Delta\}^e$ is the nodal displacement vector of the element. They are of the following forms:

$$[N] = \left[[N_1]\ [N_2]\ [N_3]\ [N_4]\ [N_5]\ [N_6]\ [N_7]\ [N_8]\ [N_9]\ [N_{10}]\ [N_{11}]\ [N_{12}] \right], \quad (5.53)$$

$$\{\Delta\}^e = \left\{ \{\Delta_1\}\ \{\Delta_2\}\ \{\Delta_3\}\ \{\Delta_4\}\ \{\Delta_5\}\ \{\Delta_6\}\ \{\Delta_7\}\ \{\Delta_8\}\ \{\Delta_9\}\ \{\Delta_{10}\}\ \{\Delta_{11}\}\ \{\Delta_{12}\} \right\}^T, \quad (5.54)$$

where $\left[N_q\right]$ and $\left\{\Delta_q\right\}$ are the corresponding submatrix and subvector related to the node q ($q = 1, 2, \ldots, 12$) of the three-dimensional 12-node dynamic infinite element. They can be expressed as follows:

$$\left[N_q\right] = \begin{bmatrix} N_q & 0 & 0 \\ 0 & N_q & 0 \\ 0 & 0 & N_q \end{bmatrix} \qquad (q = 1,2,\ldots,12), \quad (5.55)$$

$$\left\{\Delta_q\right\} = \begin{Bmatrix} u_q \\ v_q \\ w_q \end{Bmatrix} \qquad (q = 1,2,\ldots,12), \quad (5.56)$$

where N_q ($q = 1, 2, \ldots, 12$) is the displacement shape function of node q; u_q, v_q and w_q ($q = 1, 2, \ldots, 12$) are the displacement components of node q in the x, y and z directions, respectively.

Using the above definitions, the strain matrix of the three-dimensional 12-node dynamic infinite element can be expressed as follows:

$$\{\varepsilon\}^e = \begin{Bmatrix} \varepsilon_x \\ \varepsilon_y \\ \varepsilon_z \\ \gamma_{xy} \\ \gamma_{yz} \\ \gamma_{zx} \end{Bmatrix} = \begin{Bmatrix} \partial u/\partial x \\ \partial v/\partial y \\ \partial w/\partial z \\ \partial u/\partial y + \partial v/\partial x \\ \partial v/\partial z + \partial w/\partial y \\ \partial w/\partial x + \partial u/\partial z \end{Bmatrix} = [B]\{\Delta\}^e, \quad (5.57)$$

where $[B]$ is the strain matrix of the three-dimensional 12-node dynamic infinite element; and $\{\varepsilon\}^e$ is the strain vector of the element. The strain matrix of the three-dimensional 12-node dynamic infinite element can be further expressed as

$$[B] = \left[[B_1]\ [B_2]\ [B_3]\ [B_4]\ [B_5]\ [B_6]\ [B_7]\ [B_8]\ [B_9]\ [B_{10}]\ [B_{11}]\ [B_{12}] \right], \quad (5.58)$$

where $\left[B_q\right]$ is the corresponding strain submatrix related to the node q ($q = 1, 2, \ldots, 12$) of the three-dimensional 12-node dynamic infinite element. It can be expressed as follows:

$$\left[B_q\right] = \begin{bmatrix} \partial N_q/\partial x & 0 & 0 \\ 0 & \partial N_q/\partial y & 0 \\ 0 & 0 & \partial N_q/\partial z \\ \partial N_q/\partial y & \partial N_q/\partial x & 0 \\ 0 & \partial N_q/\partial z & \partial N_q/\partial y \\ \partial N_q/\partial z & 0 & \partial N_q/\partial x. \end{bmatrix} \qquad (q = 1, 2, \ldots, 12). \tag{5.59}$$

To evaluate the strain matrix of the three-dimensional 12-node dynamic infinite element, it is necessary to calculate the first derivatives of the displacement shape functions with respect to the local ξ, η and ζ coordinates as follows:

$$\frac{\partial N_q}{\partial \xi} = \frac{\partial N_q}{\partial x}\frac{\partial x}{\partial \xi} + \frac{\partial N_q}{\partial y}\frac{\partial y}{\partial \xi} + \frac{\partial N_q}{\partial z}\frac{\partial z}{\partial \xi} \qquad (q = 1, 2, \ldots, 12), \tag{5.60}$$

$$\frac{\partial N_q}{\partial \eta} = \frac{\partial N_q}{\partial x}\frac{\partial x}{\partial \eta} + \frac{\partial N_q}{\partial y}\frac{\partial y}{\partial \eta} + \frac{\partial N_q}{\partial z}\frac{\partial z}{\partial \eta} \qquad (q = 1, 2, \ldots, 12), \tag{5.61}$$

$$\frac{\partial N_q}{\partial \zeta} = \frac{\partial N_q}{\partial x}\frac{\partial x}{\partial \zeta} + \frac{\partial N_q}{\partial y}\frac{\partial y}{\partial \zeta} + \frac{\partial N_q}{\partial z}\frac{\partial z}{\partial \zeta} \qquad (q = 1, 2, \ldots, 12). \tag{5.62}$$

Equations (5.60), (5.61) and (5.62) can be readily expressed in the following matrix form:

$$\begin{aligned} \begin{Bmatrix} \partial N_q/\partial \xi \\ \partial N_q/\partial \eta \\ \partial N_q/\partial \zeta \end{Bmatrix} &= \begin{bmatrix} \partial x/\partial \xi & \partial y/\partial \xi & \partial z/\partial \xi \\ \partial x/\partial \eta & \partial y/\partial \eta & \partial z/\partial \eta \\ \partial x/\partial \zeta & \partial y/\partial \zeta & \partial z/\partial \zeta \end{bmatrix} \begin{Bmatrix} \partial N_q/\partial x \\ \partial N_q/\partial y \\ \partial N_q/\partial z \end{Bmatrix} \\ &= [J] \begin{Bmatrix} \partial N_q/\partial x \\ \partial N_q/\partial y \\ \partial N_q/\partial z \end{Bmatrix} \qquad (q = 1, 2, \ldots, 12), \end{aligned} \tag{5.63}$$

where the matrix $[J]$, called the Jacobian matrix, is given by the following equation:

$$[J] = \begin{bmatrix} \partial x/\partial \xi & \partial y/\partial \xi & \partial z/\partial \xi \\ \partial x/\partial \eta & \partial y/\partial \eta & \partial z/\partial \eta \\ \partial x/\partial \zeta & \partial y/\partial \zeta & \partial z/\partial \zeta \end{bmatrix}. \tag{5.64}$$

Substituting Eqs. (5.9), (5.10) and (5.11) into Eq. (5.64) yields the final expression for the Jacobian matrix as follows:

$$[J] = \begin{bmatrix} \sum_{q=1}^{8} \left[\left(\partial M_q/\partial \xi\right) x_q\right] & \sum_{q=1}^{8} \left[\left(\partial M_q/\partial \xi\right) y_q\right] & \sum_{q=1}^{8} \left[\left(\partial M_q/\partial \xi\right) z_q\right] \\ \sum_{q=1}^{8} \left[\left(\partial M_q/\partial \eta\right) x_q\right] & \sum_{q=1}^{8} \left[\left(\partial M_q/\partial \eta\right) y_q\right] & \sum_{q=1}^{8} \left[\left(\partial M_q/\partial \eta\right) z_q\right] \\ \sum_{q=1}^{8} \left[\left(\partial M_q/\partial \zeta\right) x_q\right] & \sum_{q=1}^{8} \left[\left(\partial M_q/\partial \zeta\right) y_q\right] & \sum_{q=1}^{8} \left[\left(\partial M_q/\partial \zeta\right) z_q\right] \end{bmatrix}. \tag{5.65}$$

Therefore, the first derivatives of the displacement shape functions with respect to the global x, y and z coordinates can be expressed as follows:

$$\begin{Bmatrix} \partial N_q/\partial x \\ \partial N_q/\partial y \\ \partial N_q/\partial z \end{Bmatrix} = [J]^{-1} \begin{Bmatrix} \partial N_q/\partial \xi \\ \partial N_q/\partial \eta \\ \partial N_q/\partial \zeta \end{Bmatrix}. \qquad (q = 1, 2, \ldots, 12). \tag{5.66}$$

Mathematically, the value of the Jacobian determinant $|J|$ can be determined from the Jacobian matrix $[J]$.

For three-dimensional solids with hysteretic damping, the constitutive matrix of the element material can be expressed in the following form:

$$\left[D^*\right] = \frac{E(1+i\eta_d)}{(1+\mu)(1-2\mu)} \begin{bmatrix} 1-\mu & \mu & \mu & 0 & 0 & 0 \\ \mu & 1-\mu & \mu & 0 & 0 & 0 \\ \mu & \mu & 1-\mu & 0 & 0 & 0 \\ 0 & 0 & 0 & (1-2\mu)/2 & 0 & 0 \\ 0 & 0 & 0 & 0 & (1-2\mu)/2 & 0 \\ 0 & 0 & 0 & 0 & 0 & (1-2\mu)/2 \end{bmatrix}, \tag{5.67}$$

where E and μ are the elastic modulus and Poisson's ratio of the element material, respectively; η_d is the hysteretic damping coefficient of the element material.

Substituting Eqs. (5.53), (5.58) and (5.67) into Eqs. (5.50) and (5.51) yields the following generalized integral for the evaluation of the mass and stiffness matrices of the three-dimensional 12-node dynamic infinite element:

$$I = \int_0^\infty F(\xi) \exp\left[-(2\alpha + i\beta_q + i\beta_r)\xi\right] d\xi \qquad (q = 1, 2, 3;\ r = 1, 2, 3). \tag{5.68}$$

To evaluate the generalized integral using the numerical integration technique (Chow and Smith 1981; Zhang and Zhao 1987), the following definition

$$\beta = \frac{\beta_q + \beta_r}{2} \qquad (q = 1, 2, 3;\ r = 1, 2, 3) \tag{5.69}$$

is introduced. As a result, Eq. (5.68) can be evaluated using the numerical integration technique described in Sect. 2.1.1.

5.3 Verification of Three-Dimensional Dynamic Infinite Elements

The first numerical example for verifying the proposed three-dimensional 12-node dynamic infinite element is to simulate the dynamic response of a square massless rigid plate resting on a homogeneous, isotropic and elastic half-space. If the square massless plate is rigid, the analytical solutions for the compliance of the plate are available (Wong and Luco 1976; Hamidzadeh-Eraghi and Grootenhuis 1981). In the process of deriving the analytical solutions, the rigid plate is considered by

assuming that the whole plate has the same translational and rotational deformations. This means that an elastic modulus of infinity is equivalently used in the related theoretical analysis. However, from the computational point of view, the elastic modulus of a finite value needs to be used for simulating the plate. To compare the emerging numerical results with the analytical solutions, the value of the elastic modulus of the plate must be several orders higher than that of the underlying rock in the coupled computational model of three-dimensional finite and dynamic infinite elements (Zhao et al. 1989, 1992, 1993d). This implies that only a "relatively rigid" plate is simulated in the corresponding computational models.

Figure 5.3 shows the computational model of a square massless plate resting on a homogeneous, isotropic and elastic half-space, in which only a quarter of the plate-foundation system is simulated using three-dimensional finite and dynamic infinite elements due to the symmetrical nature of the problem. The symmetry boundary condition is applied to the xz (i.e. $y= 0$) and yz (i.e. $x= 0$) planes for the vertical vibration of the square massless plate, while the symmetry boundary condition is applied to the xz (i.e. $y= 0$) plane and the anti-symmetry boundary condition is applied to the yz (i.e. $x= 0$) plane for the horizontal and rocking vibration of the square massless plate. To compare the current numerical results with the previous solutions (Wong and Luco 1976; Hamidzadeh-Eraghi and Grootenhuis 1981), the same assumptions as those used in the previous work are adopted for the coupled computational model of three-dimensional finite and dynamic infinite elements (Zhao et al. 1989, 1992, 1993d).

The following parameters are used in the coupled computational model of the plate-foundation system. For the rock foundation, the elastic modulus (E_r) is 24×10^9 Pa; the value of Poisson's ratio (ν_r) is 1/3; the rock density (ρ_r) is $2400\,\mathrm{kg\,m^{-3}}$. For the square massless plate, the elastic modulus (E_p) is 24×10^{12} Pa so that the plate is "relatively rigid" to the rock foundation; the half-width of the

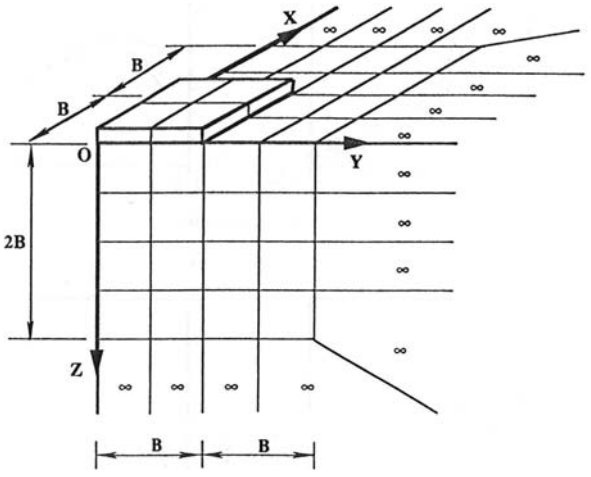

Fig. 5.3 Computational model of a massless plate resting on a homogeneous, isotropic and elastic half-space: the near field is simulated using plate and solid finite elements, while the far field is simulated using dynamic infinite elements

plate (B) is 10 m; the thickness of the plate is $B/10$. According to these parameters, the decay factor (α) used in the three-dimensional dynamic infinite elements is assumed to be 0.028, while the P-wave, S-wave and R-wave velocities, which can be determined from elastic wave theory (Graff 1975), are 3872, 1936 and 1804m s^{-1} in the rock foundation, respectively. Based on these wave velocities and the harmonic circular frequency of excitation, the three wavenumbers used in the three-dimensional dynamic infinite elements can be evaluated.

In the coupled computational model of the plate-foundation system, the square massless plate is simulated either by thick plate elements or by a combination of thick plate elements and plane stress elements (Hamidzadeh-Eraghi and Grootenhuis 1981). The near field of the rock foundation is simulated using three-dimensional eight-node solid finite elements, while the far field of the rock foundation is simulated using three-dimensional 12-node dynamic infinite elements. The resulting numerical solutions are compared with the "exact" solutions of Wong and Luco (1976), Hamidzadeh-Eraghi and Grootenhuis (1981) using the following parameters:

$$C_{HH}(a_0) = \frac{GB\Delta_1}{P_0}, \tag{5.70}$$

$$C_{VV}(a_0) = \frac{GB\Delta_3}{P_0}, \tag{5.71}$$

$$C_{MM}(a_0) = \frac{GB^3\theta_x}{M_x}, \tag{5.72}$$

$$C_{HM}(a_0) = \frac{GB^2\Delta_1}{M_x}, \tag{5.73}$$

where C_{HH} and C_{VV} are the dimensionless compliances of the plate due to the concentrated dynamic load (P_0) applied at the plate centre in the x and z directions, respectively; Δ_1 and Δ_3 are the corresponding complex displacements of the plate in the x and z directions; C_{MM} and C_{HM} are the dimensionless compliances of the plate due to the dynamic moment (M_x) applied at the plate centre; θ_x is the rotation angle of the plate corresponding to the applied moment (M_x) with respect to the x axis; G is the shear modulus of the rock foundation; a_0 is a dimensionless frequency with the following definition:

$$a_0 = \frac{\omega B}{C_S}, \tag{5.74}$$

where ω is the circular frequency of the excitation load; C_s is the S-wave velocity in the rock foundation.

Figure 5.4 shows the comparison between the current numerical results and the previous ones. In this figure, the solid and dashed lines, which are used for the representation of C_{HH} and C_{VV}, are cited from the work carried out by Wong and Luco (1976), while the solid and dashed lines, which are used for the representation of C_{MM} and C_{HM}, are cited from the work carried out by Hamidzadeh-Eraghi

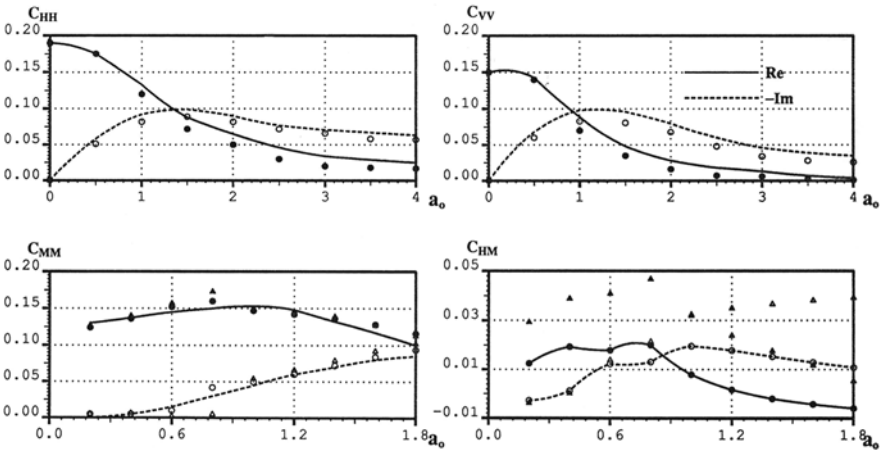

Fig. 5.4 Comparison of current results with previous results (Massless plate resting on a homogeneous, isotropic and elastic half-space)

and Grootenhuis (1981). For the computation of C_{MM} and C_{HM}, Poisson's ratio of the rock foundation is assumed to be 0.25 so that the corresponding wavenumbers for the P-wave, S-wave and R-wave need to be changed accordingly in the three-dimensional 12-node dynamic infinite elements. The solid dots and circles are used to express the numerical results obtained from the coupled computational model, in which the plate is simulated using a combination of thick plate elements and plane stress elements, while the solid triangles and hollow triangles are used to express the numerical results obtained from the coupled computational model, in which the plate is simulated only using thick plate elements. There is good agreement between the current numerical results and the previous ones when the plate is simulated using a combination of thick plate elements and plane stress elements, indicating that the accurate numerical results can be obtained from the coupled computational model of three-dimensional finite (plate) elements and dynamic infinite elements. However, when the plate is subjected to either a horizontal or a rocking loading and simulated only using thick plate elements, a significant discrepancy between the current numerical results and the previous ones is observed because the sway modes of the plate cannot be appropriately simulated by thick plate elements alone. Therefore, it is recommended that in the seismic analysis of a plate subjected to horizontal earthquakes, shell elements or a combination of thick plate elements and plane stress elements be used in the coupled computational model of three-dimensional finite (plate) elements and dynamic infinite elements.

The second numerical example for verifying the proposed three-dimensional 12-node dynamic infinite element is to simulate the dynamic response of a square massless plate resting on a visco-elastic layered foundation. This example, in essence, belongs to a wave propagation problem in a non-homogeneous infinite foundation. Figure 5.5 shows the computational model of the plate-foundation

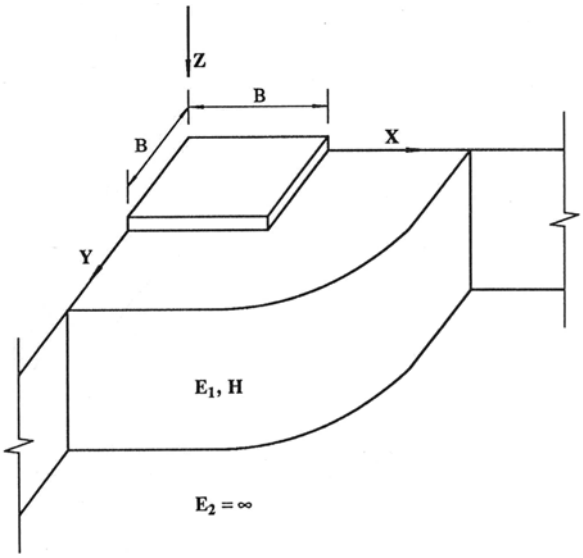

Fig. 5.5 Computational model of a massless plate resting on a layered foundation: the near field is simulated using plate and solid finite elements, while the far field is simulated using dynamic infinite elements

system. Owing to the symmetrical nature of the plate-foundation system, only a quarter of the plate-foundation system is simulated using three-dimensional finite (plate) elements and dynamic infinite elements. The same parameters as those used for the first verification example are employed in the computational model of the plate and layered foundation system. Since a layer resting on the rigid base rock is considered, the ratio of the layer depth to the plate width is assumed to be 2 in the coupled computational model of three-dimensional finite (plate) elements and dynamic infinite elements.

Figure 5.6 shows the comparison between the current numerical results with the previous ones (Chow 1987). In this figure, K and C are the dynamic stiffness coefficient and damping coefficient of the plate, respectively. The solid line is used to express the previous results (Chow 1987), while the solid dots are used to express the current numerical results obtained from the coupled computational model of three-dimensional finite (plate) elements and dynamic infinite elements. Generally, there is good agreement between the current numerical results and the previous ones, indicating that accurate numerical results can be obtained from the application of the coupled computational model of three-dimensional finite (plate) elements and dynamic infinite elements for solving three-dimensional wave-propagation problems in layered infinite foundations. Note that if the foundation of a plate/structure can be treated as a homogeneous, isotropic and visco-elastic half-space, the previous analytical and semi-analytical methods are computationally cheaper, compared with the coupled computational model used in this chapter. However, if the foundation of a plate/structure can be only treated as a non-homogeneous infinite medium, the previous analytical procedures (Wong and Luco 1976; Brebbia 1978; Hamidzadeh-Eraghi and Grootenhuis 1981; Chow 1987) are no longer directly applicable for

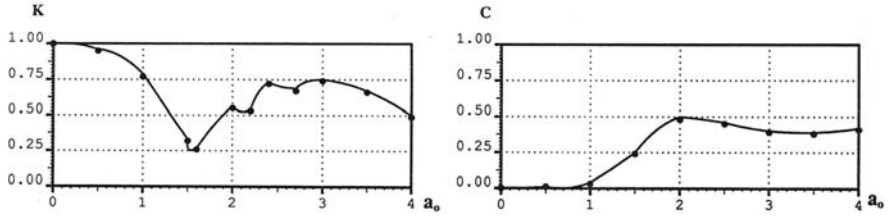

Fig. 5.6 Comparison of current results with previous results (massless plate resting on a layered foundation): the *solid lines* represent the previous solutions, while the *solid dots* represent the current results

dealing with dynamic plate/structure–foundation interaction problems, especially when dealing with dynamic arch dam—foundation interaction problems. In this case, the coupled computational model of three-dimensional finite (plate) elements and dynamic infinite elements can still work well through simply altering the parameters of different material regions, which are simulated by the three-dimensional finite (plate) elements and dynamic infinite elements.